Langmuir

Article

pubs.acs.org/Langmuir

Simulation Analysis of Contact Angles and Retention Forces of Liquid Drops on Inclined Surfaces

M. J. Santos, S. Velasco, and J. A. White*,†

Departamento de Física Aplicada, Universidad de Salamanca, 37008 Salamanca, Spain

ABSTRACT: A simulation study of liquid drops on inclined surfaces is performed in order to understand the evolution of drop shapes, contact angles, and retention forces with the tilt angle. The simulations are made by means of a method recently developed for dealing with contact angle hysteresis in the public-domain Surface Evolver software. The results of our simulations are highly dependent on the initial contact angle of the drop. For a drop with an initial contact angle equal to the advancing angle, we obtain results similar to those of experiments in which a drop is placed on a horizontal surface that is slowly tilted. For drops with an initial contact angle equal to the mean between the advancing and the receding contact angles, we recover previous results of finite element studies of drops on inclined surfaces. Comparison with experimental results for molten Sn−Ag−Cu on a tilted Cu substrate shows excellent agreement.

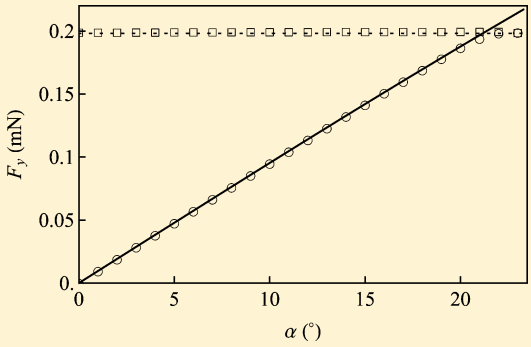

INTRODUCTION

The Young−Laplace equation[1,2] determines that a drop on a horizontal surface has an axisymmetric shape due to cylindrical symmetry. This shape becomes nonaxisymmetric when the surface is tilted (or rotated at a given angular speed). For tilt angles α below a critical value α_c, one observes that the drop remains adhered to the surface because of a change in shape: the drop leans in the direction of inclination so that the contact angles in the front are larger than those in the rear. The difference between the contact angles in the drop is called contact angle hysteresis and gives rise to a capillary retention force that balances gravity and avoids the movement of the drop.

The study of the retention of liquid drops resting on inclined surfaces has been the subject of much research since the seminal inspiring paper of MacDougall and Ockrent in 1942.[3] These authors determined that the product of the area A of the drop cross-section times sin α is proportional to the difference between the cosines of the contact angles at the rear (receding) edge and at the front (advancing) edge of the drop

$$\rho g A \sin \alpha = \sigma_{lv}(\cos \theta_{rear} - \cos \theta_{front}) \quad (1)$$

where ρ is the liquid density, g is the acceleration of gravity, and σ_{lv} is the liquid−vapor surface tension. It should be emphasized here that eq 1 considers drops at different, noncritical inclinations and thus, in general, θ_{rear} and θ_{front} are different from the receding and advancing contact angles θ_{rec} and θ_{adv} characteristic of the critical inclination at which the drop begins to slide. Of course, MacDougall and Ockrent[3] noted that eq 1 becomes

$$\rho g A \sin \alpha_c = \sigma_{lv}(\cos \theta_{rec} - \cos \theta_{adv}) \quad (2)$$

at critical tilt angle. For a given system, this implies that $A \sin \alpha_c$ is independent of drop size. Bikerman[4] noted that because the drop volume V is roughly equal to $2\omega A$, where 2ω is the width of the drop in the direction perpendicular to inclination, this also implies that $mg \sin \alpha_c/\omega = \rho g V \sin \alpha_c/\omega$ should be independent of drop size. Furthermore, eq 2 suggests that this ratio should be proportional to the cosine difference $\cos \theta_{rec} - \cos \theta_{adv}$. This fact was observed by Furmidge,[5] who showed that for parallel-sided drops at critical inclinations one has

$$\frac{\rho g V \sin \alpha_c}{\sigma_{lv}} = k\omega(\cos \theta_{rec} - \cos \theta_{adv}) \quad (3)$$

where the retention-force factor k is equal to 2.

Several tests and variations of eq 3 have been proposed in the literature using theoretical, numerical, and experimental arguments and assuming different shapes for the contact line. Larkin[6] checked eq 3 against the results obtained from numerical calculations of drop shapes, finding disagreements that were ascribed to the fact that Larkin calculations were made for static drops whereas eq 3 applies for sliding drops. Wolfram and Faust[7] considered drops with fixed circular contact lines of radius R (in this case, $\omega = R$) obtaining $k = \pi$. Using finite element methods, Brown et al.[8] also considered a fixed circular contact line but found a value of $k = \pi/2$ for the retention-force factor. Dussan and Chow[9,10] considered a contact line formed by two semicircular arcs joined by two parallel sides along the direction of inclination as an approximation for sliding drops. Assuming constant contact angles for the arc at the front (θ_{adv}) and the rear (θ_{rec}) of the

Received: May 11, 2012
Revised: June 29, 2012
Published: July 19, 2012

   dx.doi.org/10.1021/la3019293 | *Langmuir* 2012, 28, 11819−11826

drop, they obtained the result of Furmidge[5] (i.e., eq 3 with k = 2). Extrand and co-workers[11,12] performed experimental studies of critical drops, finding that for low hysteresis ($(\theta_{adv} - \theta_{rec})/\theta_{adv}$ small) the drop contact line was nearly circular, and good agreement was found with eq 3 with $\omega = R$ and $k = {}^4/_{\pi}$.[11] For high hysteresis, the drop contact line was elongated, and it was found that the value of k increased with elongation, approaching k = 2 only for relatively large hysteresis.[12] Recently, ElSherbini and Jacobi[13] proposed a variation of eq 3 in which ω was replaced by the equivalent radius R_A of a circle with the same area as that of the drop base, and a value of $48/\pi^3$ was obtained for the retention-force factor k. Very recent experiments of Bouteau et al.[14] have found that the sliding behavior of droplets on inclined Langmuir–Blodgett surfaces is reasonably well described by the Furmidge model of eq 3 with k = 2.

In many cases, the above-mentioned discrepancies are due to the use of different theoretical assumptions or different conditions for the experiments. For instance, the experiments of Quéré et al.[15] and of ElSherbini and Jacobi[13,16,17] were performed by placing a droplet on an inclined surface whereas those of Extrand and co-workers considered either a drop on a horizontal surface that was subsequently tilted[12] or a drop on a spinning platter.[11] Pierce et al.[18] studied different tilted plate experimental methods, obtaining significant deviations in the critical tilt angle depending on the method. Other sources of discrepancies can be due to the time the drop was resting on the surface prior to motion[19] or to the initial contact angle that the drop adapts as a result of its placement on the surface.[18,20] From a theoretical viewpoint, some researchers considered a fixed circular contact line[8] and others assumed sliding, parallel-sided drops.[9,10] More recent numerical works have considered simulation schemes in which the contact line is allowed to move using a finite-elements method[21,22] or an optimization-problem approach.[23] In 2005, Krasovitski and Marmur[24] considered a theoretical study of drops in two dimensions in which they showed that the maximum and minimum contact angles for drops on an inclined plane did not always coincide with the advancing and receding contact angles.

The goal of the present work is to try to shed some light on the problem by considering simulations of drops on inclined surfaces by means of a simulation scheme for modeling contact angle hysteresis in the Surface Evolver framework,[25] which was recently developed by us.[26] The method is valid for nonaxisymmetric drops and therefore can be applied to the problem of drops on inclined surfaces. Of course, using this method one can perform measurements both for critical and noncritical drops. This will allow us to analyze the evolution toward the critical tilt angle for different initial conditions of the simulation.

This work is structured as follows. We start with a brief summary of the method for simulating drops on inclined surfaces. Then we consider the evolution of a drop on a horizontal surface that is slowly tilted for two different initial situations: (i) an initial contact angle equal to θ_{adv} and (ii) an initial contact angle equal to $(\theta_{rec} + \theta_{adv})/2$. Next we compare with experimental data for molten Sn–Ag–Cu on a tilted Cu substrate. We conclude with a brief summary of this work.

SIMULATION METHOD

The shape of a sessile drop under gravity $\mathbf{g}$ with a Young contact angle of θ_Y can be obtained by minimizing the energy functional[26]

$$U = \sigma_{lv}A_{lv} - \int\int_{A_{ls}} \sigma_{lv}\cos\theta_Y \, dA - \int\int\int_V \Delta\rho \mathbf{g} r \, dV \tag{4}$$

subjected to a fixed volume V constraint. In eq 4, A_{ls} is the area of the liquid in contact with the surface (the area of the drop base), A_{lv} is the area of the liquid–vapor interface, and $\Delta\rho$ represents the difference in density of liquid and vapor phases ($\Delta\rho \approx \rho$, the liquid density).

A finite-element method for solving the variational problem of eq 4 is provided by the Surface Evolver software by Brakke,[25] which was specially designed for finding the minimal surface (of the drop) subjected to a set of constraints. The drop surface is represented in Surface Evolver by a tessellation with triangular facets joined by edges ending in vertices. A direct way of implementing a tilt angle in Surface Evolver is to consider an inclined gravity vector $\mathbf{g} = (0, g\sin\alpha, g\cos\alpha)$ so that for $\alpha = 0$ one recovers a gravity acceleration of g in the z (vertical) direction. For $\alpha \neq 0$, one obtains a nonzero contribution in the y direction (the direction of inclination). Minimizing eq 4 with Surface Evolver for an inclined surface ($\alpha \neq 0$) would lead to a drop moving in the y direction with acceleration $g\sin\alpha$ because the functional of eq 4 does not include a capillary retention term based on contact angle hysteresis that could balance gravity in the direction of tilt. Very recently,[26] we developed an algorithm for including contact angle hysteresis in Surface Evolver that allows us to minimize eq 4 properly for an inclined surface by adding local constraints in the variational approach. For clarity, we sketch here the main steps of the algorithm; more details can be found in the original paper:[26]

(1) At the beginning of the iteration loop, the coordinates of vertices i that belong to the contact line are stored: $\vec{x}_{i,old} = \vec{x}_i$.

(2) A virtual displacement of the drop is made to obtain the new coordinates of the contact line vertices $\vec{x}_i = \vec{x}_{i,new}$ and to calculate the dimensionless force per unit length f_i/σ_{lv} acting on each of these vertices. This force is obtained in Surface Evolver by projecting the vertex displacement over the normal to the contact line and dividing by the mean length of the two edges attached to it that belong to the contact line. The sign of the projection indicates whether the vertex is in an advancing situation or in a receding one.

(3) For each advancing vertex, $|f_i|$ is compared to the maximum advancing force per unit length

$$f_{adv} = \sigma_{lv}(\cos\theta_Y - \cos\theta_{adv}) \tag{5}$$

where θ_Y is the Young contact angle. In this work, for θ_Y we shall make the usual assumption:

$$\theta_Y = \frac{\theta_{rec} + \theta_{adv}}{2} \tag{6}$$

We note that recent experiments show that this assumption is close to the most-stable contact angle of the drop,[27,28] although other choices for θ_Y are possible.[29] Another common assumption for θ_Y is given by

$$\cos\theta_Y = \frac{\cos\theta_{rec} + \cos\theta_{adv}}{2} \tag{7}$$

Our simulations show very small differences between the results obtained from eqs 6 and 7.

If $|f_i| \le f_{adv}$, then vertex i is kept fixed ($\vec{x}_i = \vec{x}_{i,old}$). Conversely, if $|f_i| > f_{adv}$, then vertex is allowed to move according to the following expression:

$$\vec{x}_i = \vec{x}_{i,old} + (\vec{x}_{i,new} - \vec{x}_{i,old})\frac{|f_i| - f_{adv}}{|f_i|} \quad (8)$$

(4) Analogously, for each receding vertex $|f_i|$ is compared to the maximum receding force per unit length

$$f_{rec} = \sigma_{lv}(\cos\theta_{rec} - \cos\theta_Y) \quad (9)$$

where we note that assumption 7 leads to $f_{rec} = f_{adv}$.[26]

If $|f_i| \le f_{rec}$, then the vertex position is retained ($\vec{x}_i = \vec{x}_{i,old}$). If $|f_i| > f_{rec}$, then the vertex is allowed to move according to

$$\vec{x}_i = \vec{x}_{i,old} + (\vec{x}_{i,new} - \vec{x}_{i,old})\frac{|f_i| - f_{rec}}{|f_i|} \quad (10)$$

(5) The above steps are iterated until convergence is reached.

The preceding algorithm allows us to calculate both the shape of a drop on an inclined surface and the capillary retention forces acting on each vertex of the contact line. The contact angles can also be accurately measured via[26]

$$\theta_i = \begin{cases} \theta_{adv} & \text{if } |f_i| \ge f_{adv} \\ \arccos(\cos\theta_Y - |f_i|/\sigma_{lv}) & \text{if } |f_i| < f_{adv} \end{cases} \quad (11)$$

for an advancing vertex and

$$\theta_i = \begin{cases} \theta_{rec} & \text{if } |f_i| \ge f_{adv} \\ \arccos(\cos\theta_Y + |f_i|/\sigma_{lv}) & \text{if } |f_i| < f_{adv} \end{cases} \quad (12)$$

for a receding one.

SIMULATION OF A TILT PROCESS

In this section, we shall simulate the process in which an initially horizontal plane is slowly tilted until it reaches the critical tilt angle for a drop resting on it. To perform such a simulation with the algorithm presented in the preceding section, we require only a few input parameters to describe the drop shape, retention forces, and contact angles. For a liquid drop on a given surface, these input parameters are the drop volume V, the surface tension σ_{lv}, the liquid density ρ, and the advancing and receding contact angles for the system. We recall here that, according to the results of Krasovitski and Marmur,[24] the advancing and receding contact angles for drops on an inclined substrate can differ from the usual advancing and receding contact angles. Additionally, one must establish the initial conditions for the system. We shall consider two different initial conditions: (i) initial contact angle equal to θ_{adv} and (ii) initial contact angle equal to θ_Y.

Initial Contact Angle Equal to θ_{adv}. We consider an initial contact angle equal to θ_{adv} for a drop placed on a horizontal surface that is subsequently tilted because this situation resembles the usual experimental conditions.[18] This situation has also been considered in a very recent work by Chou et al.[30]

First, to test our simulation procedure, we begin with an analysis of the retention forces arising in the triple contact line. Because the retention force acting on each vertex of the triple line can be measured in the Surface Evolver simulation, it is direct to obtain the total retention force along the tilt direction, F_y. For a noncritical drop, this total retention force must balance the gravity contribution $\rho g V \sin\alpha$. This balance should provide a convergence test for the simulation because an equilibrium situation is reached only when these two terms cancel each other.

Figure 1 compares the total retention force with the gravity contribution for a drop of water of volume $V = 0.056$ cm^3 on an inclined PCTFE surface.[12] In the simulation, we have considered the advancing and receding contact angles obtained by Extrand and Kumagai[12] for this system (i.e., $\theta_{adv} = 99.6°$ and $\theta_{rec} = 73.6°$). In this case, the simulation has been done by starting from an axisymmetric drop with an initial contact angle equal to θ_{adv} that is placed on a horizontal surface ($\alpha = 0°$) and then increasing the tilt angle α in steps of $\Delta\alpha = 1°$. For each α, a total number of $N = 1000$ steps have been made in order to reach equilibration. As one can observe in Figure 1, the retention force F_y is very similar, within the numerical precision of the simulation, to the gravitation term $\rho g V \sin\alpha$ for $\alpha \lesssim 21°$, indicating that the drop is static and that the system has reached equilibrium. For $\alpha \gtrsim 21°$, the retention force approaches its maximum value and cannot balance the gravitational term. Under these circumstances, the drop slides and the simulation cannot be equilibrated. In all simulation results of the present work, we obtain the same behavior (i.e., $F_y = \rho g V \sin\alpha$ for tilt angles below α_c). Of course, above the critical angle α_c, Surface Evolver cannot correctly describe the sliding drop, and the presented results are a mere indication of the change in behavior of the system.

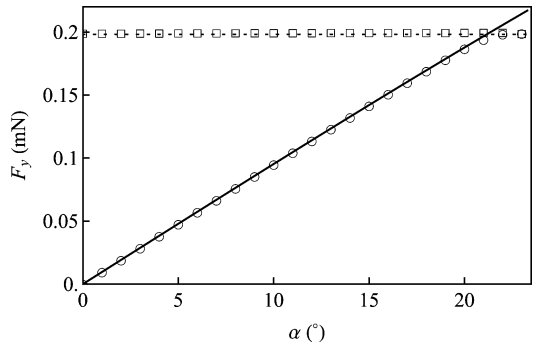

Figure 1. Force balance for a drop in a tilted plane. (−) Gravity contribution $\rho g V \sin\alpha$. (○) Total retention force along the tilt direction F_y. (···) Maximum total retention force estimated from eq 3 with $k = 2$. (□) Maximum total retention force estimated during the simulation.

The maximum value for the retention force $F_{y,max}$ can be calculated during a simulation run by obtaining the maximum retention force for each vertex of the triple line, adding these contributions, and then projecting over the tilt direction y. The values obtained for $F_{y,max}$ at each tilt angle are plotted in Figure 1 with squares. Another estimation of the maximum retention force can be made by considering the gravity contribution at the critical angle:

$$F_c = \rho g V \sin\alpha_c \quad (13)$$

Using eq 3 with $k = 2$, one obtains

$$F_c = 2\sigma_{lv}\omega(\cos\theta_{rec} - \cos\theta_{adv}) \quad (14)$$

where the value of ω can be obtained from simulation data. In our simulations, ω remains almost constant for $\alpha < \alpha_c$, and thus F_c is also constant below the critical tilt angle. In the present

dx.doi.org/10.1021/la3019293 | Langmuir 2012, 28, 11819−11826

case, we obtain F_c = 0.198241 mN. This value is plotted in Figure 1 (dotted line) with good agreement with the results for $F_{y,max}$. Furthermore, using this value in eq 13 leads to a critical tilt angle of α_c = 21.176°, which is also in good agreement with the above observations. As is well known from eqs 13 and 14, one obtains that α_c depends on the drop volume via

$$\sin \alpha_c = \frac{2\sigma_{lv}\omega(\cos \theta_{rec} - \cos \theta_{adv})}{\rho g V} \approx V^{-2/3} \quad (15)$$

where we used $\omega \approx V^{1/3}$. Furthermore, the minimum drop volume for drop sliding is readily obtained from eq 15 by taking α_c = 90°. The behavior predicted by eq 15 agrees with our simulation results. We note that, in general, in our simulations we observe that the drop starts to slide with a tilt angle slightly smaller than that coming from eq 3 with k = 2. This fact could be due to numerical instabilities during the simulation run.

The preceding results for eq 3 with k = 2 agree with our simulation results for inclinations close to the critical one, α_c. This indicates that a similar equation could be valid for inclinations lower than α_c. We propose

$$\frac{\rho g V \sin \alpha}{\sigma_{lv}\omega} = k(\cos \theta_{min} - \cos \theta_{max}) \quad (16)$$

where θ_{min} and θ_{max} are, respectively, the minimum and maximum contact angles in the drop for a given tilt angle. In general, θ_{min} and θ_{max} depend on the inclination (i.e., $\theta_{min} = \theta_{min}(\alpha)$), and the same applies for θ_{max}. We note that eq 16 with k = 1 can be obtained by replacing the area A by the ratio V/ω in eq 1. When we take into account that for $\alpha < \alpha_c$ the gravity force $\rho g V \sin \alpha_c$ balances the total retention force F_y, eq 16 leads to

$$\frac{F_y}{\sigma_{lv}\omega} = k(\cos \theta_{min} - \cos \theta_{max}) \quad (17)$$

To test eq 17, in Figure 2a we plot the dimensionless total retention force $F_y/\sigma_{lv}\omega$ versus the cosine difference Δcos = cos θ_{min} − cos θ_{max} for the system considered in Figure 1. For Δcos < Δcos θ_{max} = cos θ_{rec} − cos θ_{adv}, we obtain linear behavior in agreement with eq 17. In this case, the linear regression of the data yields a slope of k = 1.779. The maximum value of Δcos is reached for a tilt angle slightly below α = 19° (Figure 3a). Once this value is reached, $F_y/\sigma_{lv}\omega$ still increases until reaching (approximately) the value given by slope k = 2 at the critical tilt. Therefore, once the maximum value of Δcos is attained, increasing the tilt angle leads to a change in the retention force factor k in order to balance the increase in the gravitational force.

In this case in which we start our simulation with a contact angle equal to θ_{adv}, we observe that θ_{max} remains equal to θ_{adv} while θ_{min} decreases with the tilt. This is shown in Figure 3a, where we observe that θ_{min} decreases linearly with α until reaching θ_{rec}. This linear behavior is closely related to eq 16. From this equation, one would expect a linear relationship between cos θ_{min} and sin α; however, in this case, this relation also applies for θ_{min} and α, given the values taken by these angles. For smaller values of θ_{min} or larger values of α, deviations from linear behavior take place, as we shall see in the forthcoming section.

Figure 4 shows the evolution with the inclination of the triple contact line (Figure 4a) and the contact angles (Figure 4b). At α = 0°, the contact line has a circular shape (dotted line in Figure 4a) and all contact angles are equal to θ_{adv} = 99.6°. For

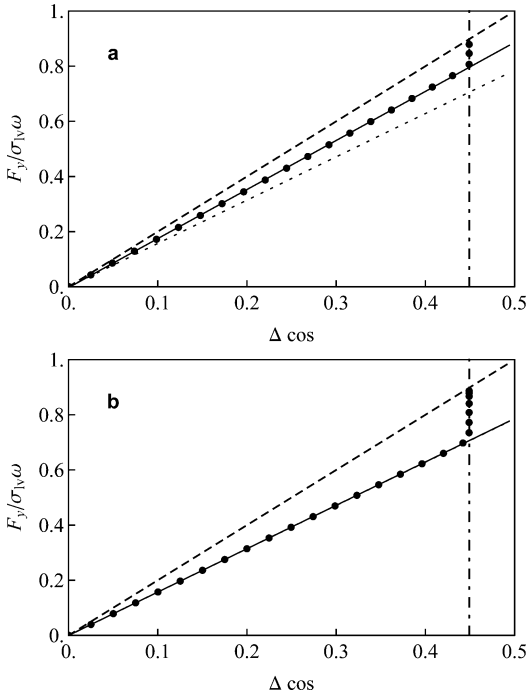

Figure 2. Dimensionless total retention force $F_y/\sigma_{lv}\omega$ vs the cosine difference Δcos = cos θ_{min} − cos θ_{max}. (a) Initial contact angle equal to θ_{adv}. (b) Initial contact angle equal to θ_Y. The symbols are simulation data. The solid lines are linear fits to the data, with slopes of (a) k = 1.779 and (b) k = 1.573 ≈ $\pi/2$. (---) Slope k = 2. (···) Slope k = $\pi/2$. The vertical dotted−dashed lines indicate Δcos$_{max}$ = cos θ_{rec} − cos θ_{adv}.

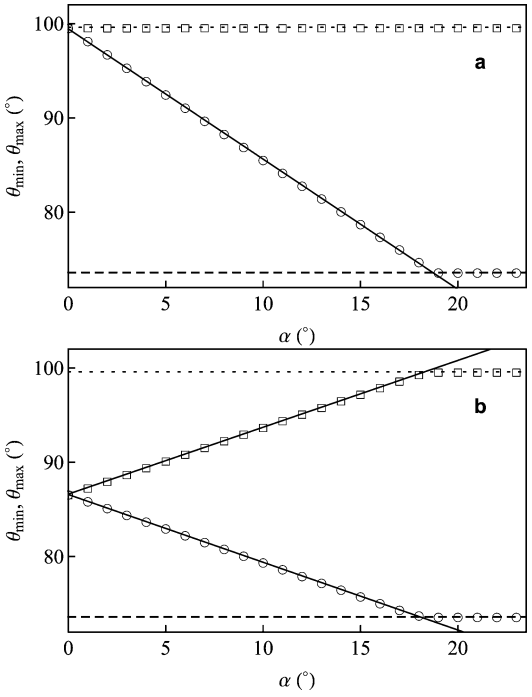

Figure 3. (○) θ_{min} and (□) θ_{max} vs the tilt angle α. (a) Initial contact angle equal to θ_{adv}. (b) Initial contact angle equal to θ_Y. The symbols are simulation data. The solid lines are linear fits to the data. The dashed and dotted lines indicate θ_{rec} and θ_{adv}, respectively.

0° < $\alpha \lesssim$ 19°, the rear of the contact line stays fixed while the front is displaced downhill. This is shown in Figure 4a for a tilt

dx.doi.org/10.1021/la3019293 | Langmuir 2012, 28, 11819−11826

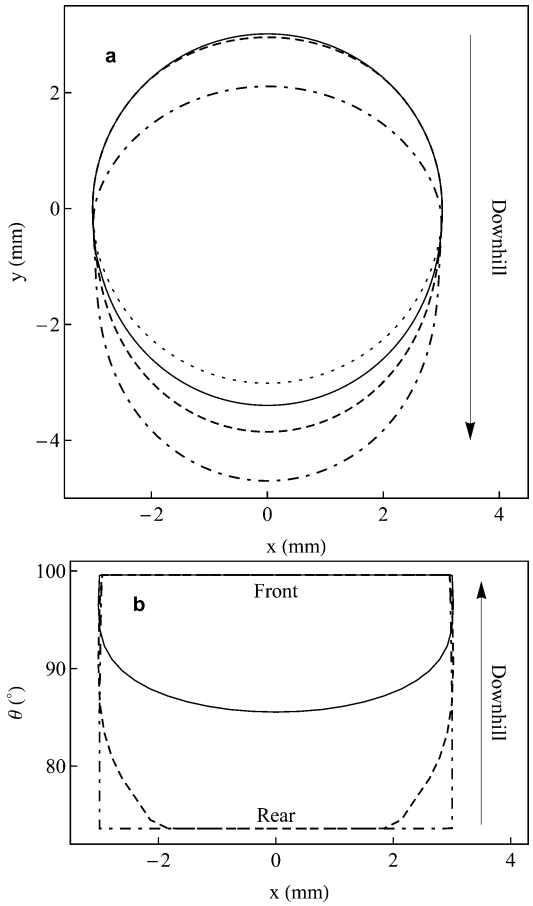

Figure 4. Surface Evolver results for drops at different tilt angles α with an initial contact angle equal to θ_{adv}. (a) Triple contact line. (b) Contact angles as a function of the coordinate x perpendicular to the inclination. (···) $\alpha = 0°$, (—) $\alpha = 10°$, (---) $\alpha = 20°$, and (·-·) $\alpha = 23°$.

angle of $\alpha = 10°$ (solid line). In Figure 4b, we show (solid line) the contact angle profile for this intermediate case and observe that whereas all contact angles at the front are equal to θ_{adv}, the contact angles in the rear are still smaller than $\theta_{rec} = 73.6°$, explaining why the rear part of the contact line remains fixed. At $\alpha = 20°$ (dashed lines), we observe in Figure 4b that part of the contact angles in the rear have attained the receding value θ_{rec}; accordingly, this part of the rear contact line is slightly displaced downhill (Figure 4a, dashed line). Because part of the contact line is still fixed, the drop is static. At $\alpha = 23°$ (dotted–dashed lines), the drop is already sliding. In this case, we note that the width of the drop becomes slightly smaller than the original and the drop tends to acquire the shape considered by Dussan and Chow,[9,10] with a contact line formed by two semicircular arcs joined by two parallel sides (Figure 4a), where the contact angles for the arc at the front are equal to θ_{adv} and those for the rear arc are equal to θ_{rec} (Figure 4b). In spite of the fact that the results for $\alpha = 23°$ agree with previous work, one has to take into account that, as mentioned previously, our simulations cannot describe a sliding drop correctly.

Initial Contact Angle Equal to θ_Y. Some recent works have considered an injection/suction procedure to prepare drops with different initial contact angles[27,28,31,30] so that one can consider a tilting experiment with a prescribed initial condition. The results of the tilting process are crucially influenced by the initial conditions of the drop, as we shall see in what follows.

Let us consider the same system as that of Figure 1 but with an initial axisymmetric drop with a contact angle equal to θ_Y. An analysis like the one performed in Figure 1 shows that the retention force F_y balances $\rho g V \sin\alpha$ for $\alpha \lesssim 23°$. For $\alpha \gtrsim 23°$, the drop slides and the simulation cannot be equilibrated. Furthermore, from eqs 13 and 14 we obtain $\alpha_c = 23.360°$ and $F_c = 0.217592$ mN. Compared to the preceding case in which $\alpha_c = 21.176°$ and $F_c = 0.198241$ mN, we note that in that case the larger initial contact angle implied a smaller drop width and therefore a smaller critical angle and retention force.

Figure 2b shows the dimensionless total retention force $F_y/\sigma_{lv}\omega$ versus the cosine difference $\Delta\cos$ for this situation with an initial contact angle equal to θ_Y. As in Figure 2a, we obtain linear behavior for $\Delta\cos < \Delta\cos_{max}$. However, in this case a linear fit of the data yields a slope of $k = 1.573 \approx \pi/2$, in accordance with the finite-element results of Brown et al. for a fixed circular contact line.[8] This agreement was expected because in our simulations the vertices belonging to the triple contact line remain fixed if their contact angles θ_i fulfill $\theta_{rec} < \theta_i < \theta_{adv}$. Therefore, starting with a circular contact line with $\theta = \theta_Y$ implies that the triple line remains circular until either $\theta_{max} = \theta_{adv}$ or $\theta_{min} = \theta_{rec}$. These two conditions are reached at approximately the same tilt angle ($\alpha \approx 18°$), as one can see in Figure 3b where one can also observe that θ_{min} (θ_{max}) decreases (increases) linearly with α until reaching θ_{rec} (θ_{adv}). The maximum value of $\Delta\cos$ is also reached for $\alpha \approx 18°$. For $\alpha > 18°$, $\Delta\cos$ remains equal to $\Delta\cos_{max}$ whereas $F_y/\sigma_{lv}\omega$ approaches its maximum value given by the slope $k = 2$ (Figure 2b) at a critical tilt angle of $\alpha \approx 23°$.

As mentioned above, the linear relation obtained for the evolution of maximum and minimum contact angles with tilt for $\Delta\cos < \Delta\cos_{max}$ is related to the linear relation between $\sin\alpha$ and $\cos\theta_{min}$ or $\cos\theta_{max}$. In particular, from eq 16, we propose

$$\frac{\rho g V \sin\alpha}{\sigma_{lv}\omega} = k_1(\cos\theta_{min} - c_1) \tag{18}$$

for θ_{min}, with k_1 and c_1 being constants. Analogously, we also propose

$$\frac{\rho g V \sin\alpha}{\sigma_{lv}\omega} = -k_2(\cos\theta_{max} - c_2) \tag{19}$$

for θ_{max}. Compared to eq 16, we obtain

$$c_1 = c_2 = \cos\theta_{initial} \tag{20}$$

and

$$k = \frac{1}{1/k_1 + 1/k_2} \tag{21}$$

In the present case, a linear fit to the data yields $c_1 = 0.05955$, $c_2 = 0.05940$, very close to $\cos\theta_Y = 0.05931$, and $k_1 = k_2 = 3.157$, which from eq 21 leads to $k = 1.5785$, which is very close to $\pi/2$, and to the slope $k = 1.573$ obtained in Figure 2b. In the preceding case where $\theta_{max} = \theta_{initial} = \theta_{adv}$ and thus $k_2 \to \infty$, we obtain $c_1 = -0.1650 \approx \cos\theta_{adv} = -0.1668$ and $k_1 = k = 1.786$, which is also very close to the value $k = 1.779$ obtained in Figure 2a.

Figure 5 shows the evolution with the inclination of the triple contact line (Figure 5a) and the contact angles (Figure 5b). At $\alpha = 0°$, the contact line has a circular shape (dotted line in Figure 5a), and all contact angles are equal to $\theta_Y = 86.6°$ (dotted line in Figure 5b). For $0° < \alpha \lesssim 18°$, the whole contact line stays fixed because all contact angles belong to the range

dx.doi.org/10.1021/la3019293 | Langmuir 2012, 28, 11819–11826

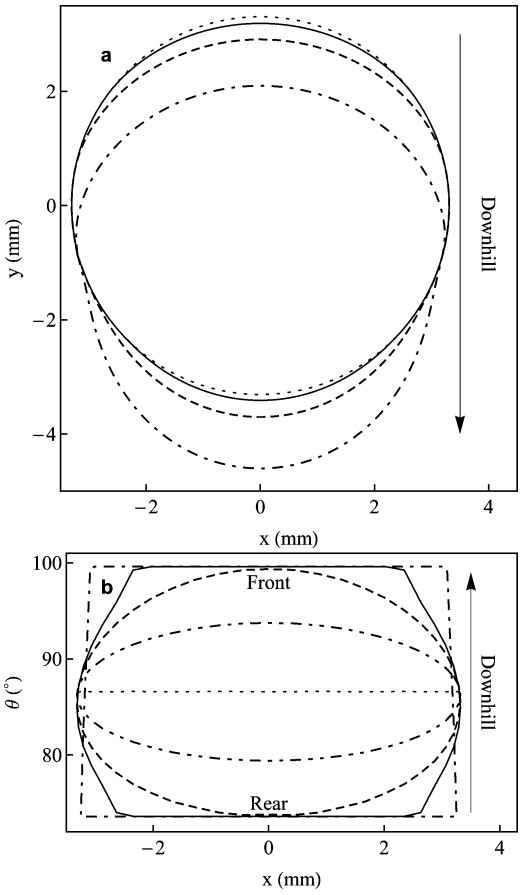

Figure 5. Surface Evolver results for drops at different tilt angles α with an initial contact angle equal to θ_Y. (a) Triple contact line. (···) $\alpha \leq 18°$, (—) $\alpha = 21°$, (---) $\alpha = 23°$, and (···) $\alpha = 25°$. (b) Contact angles as a function of the coordinate x perpendicular to the inclination. (···) $\alpha = 0°$, (·····) $\alpha = 10°$, (---) $\alpha = 18°$, (—) $\alpha = 21°$, and (·-·-) $\alpha = 25°$.

$\theta_{rec} < \theta < \theta_{adv}$. As shown in Figure 5b for $\alpha = 10$ and 18°, increasing the tilt leads to a gradual distribution of contact angles so that those in the rear decrease until reaching θ_{rec} and those in the front increase until reaching θ_{adv}, in accordance with the results presented in Figure 3b. For $18° \lesssim \alpha \lesssim 23°$, part of the contact angles in the rear have attained the receding value θ_{rec}, and this part of the contact line is displaced downhill. Analogously, part of the contact angles in the front have attained the advancing value θ_{adv}, and this part is also displaced downhill but the drops remain static. This displacement is shown in Figure 5a for $\alpha = 21$ and 23°. At $\alpha = 25°$ (Figure 5), the drop is already sliding, all front contact angles are equal to θ_{adv}, all rear contact angles are equal to θ_{rec}, and the drop width is reduced.

To conclude, in this section we have seen how the choice of the initial contact angle of the drop has a relevant effect on the obtained results. Other choices such as an initial contact angle equal to θ_{rec} are possible.[28,30] In this case, our simulation results (not shown) reveal that the front part of the contact line is initially pinned and the rear part is displaced downhill. While the front part of the contact line remains pinned, the front contact angles grow until reaching θ_{adv}, in agreement with recent results.[30]

■ COMPARISON WITH EXPERIMENTAL DATA

The goal of this section is to compare our simulation results with experimental data for the evolution of the maximum and minimum contact angles during a tilting process. In particular, we shall compare our results with the measurements of Xu et al.[32] for molten Sn 3.0 wt %−Ag 0.5 wt %−Cu (a well-known Pb-free soldering material) on tilting oxygen-free Cu in the temperature range of 490−565 K.

According to Xu et al.'s[32] data, we consider a sample of molten solder of 0.72 g with an initial contact angle of $\theta = 60.9°$, an advancing contact angle of $\theta_{adv} = 66.8°$, and a receding contact angle of $\theta_{rec} = 16.8°$. For this system, following the data of Moser et al.,[33] we also consider a density of $\rho = 7.1$ g/cm^3 and a surface tension of $\sigma_{lv} = 540$ mN/m. Prior to analyzing our simulation results, we note that, in contrast to the results in the previous section, this is a system with pronounced hysteresis in which the initial contact angle is neither θ_{adv} nor θ_Y. Consequently, some differences with the previously presented results are expected.

Figure 6a shows the evolution of θ_{min} and θ_{max} with the tilt angle α. Overall, excellent agreement is obtained between

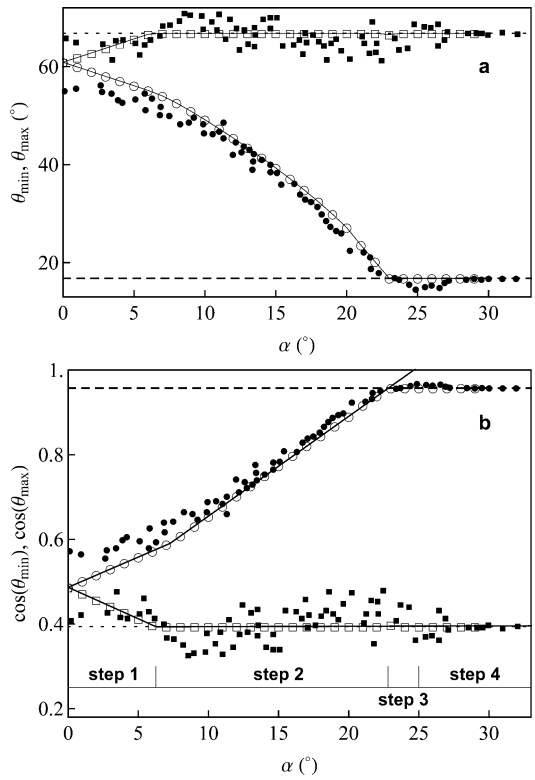

Figure 6. Comparison of simulation results and the experimental data for molten Sn−Ag−Cu on a tilted Cu substrate: (a) θ_{min} (●, ○) and θ_{max} (■, □) vs the tilt angle α. The solid lines are guides to the eye. The dashed lines and the dotted lines indicate θ_{rec} and θ_{adv}, respectively. (b) cos θ_{min} (●, ○) and cos θ_{max} (■, □) vs the tilt angle α. The solid lines are linear fits to the data. The dashed lines and the dotted lines indicate cos θ_{rec} and cos θ_{adv}, respectively. In both panels, the filled symbols are experimental data.[32]

experimental and simulation data, with the main differences being due to experimental fluctuations. Compared to the results in the preceding section, in the present situation of large hysteresis the variation in the contact angles with tilt is no longer linear. This is due to the fact that in this case the cosine

dx.doi.org/10.1021/la3019293 | Langmuir 2012, 28, 11819−11826

terms in eqs 18 and 19 cannot be linearized. Instead, if we consider cos θ_{min} and cos θ_{max}, then we recover piecewise linear behavior, as shown in Figure 6b. We remark here that from eqs 18 and 19 one expects linear relationships between the cosines of the contact angles and the sine of the tilt angle, but in the present situation, sin $\alpha \approx \alpha$ and we use the tilt angle for clarity.

Four steps are identified in the contact angle evolution presented in Figure 6.

(1) $0 < \alpha \lesssim 6.3°$: In this case, $\theta_{min} > \theta_{rec}$ and $\theta_{max} < \theta_{adv}$; consequently, the triple contact line remains fixed, with a circular profile. cos θ_{max} decreases linearly with α until reaching cos θ_{adv}. cos θ_{min} increases linearly with α. The behavior of the system is similar to the first step in Figure 3b.

(2) $6.3° \lesssim \alpha \lesssim 22.8°$: Because $\theta_{max} = \theta_{adv}$, the front of the drop is displaced downhill while the rear stays fixed. The drop shape becomes elongated. We note that at $\alpha \approx 7.3°$ the slope of cos θ_{min} changes and the behavior of the system becomes similar to that presented in Figure 3a. From $\alpha \approx 7.3°$, cos θ_{min} increases linearly until reaching cos θ_{rec} at $\alpha \approx 22.8°$.

(3) $22.8° \lesssim \alpha \lesssim 25°$: Now $\theta_{min} = \theta_{rec}$ and part of the rear contact line is displaced. The drop remains static.

(4) $\alpha \gtrsim 25°$: At $\alpha \approx 25°$, we reach the critical tilt angle and the drop slides. The simulation cannot be equilibrated and becomes unstable.

Critical tilt angles $\alpha_d \approx 6.3°$ and $\alpha_u \approx 22.8°$ indicate, respectively, where the impending motion of the downhill and uphill parts of the contact line occurs. These angles together with the critical tilt angle $\alpha_c \approx 25°$ determine the four steps in the evolution of the system. The steps above reveal a hybrid situation between the two situations considered in the preceding section. The system first behaves like that in Figure 3b and then like that in Figure 3a. Similar behavior has been obtained experimentally by Berejnov and Thorne for water drops on siliconized flat surfaces.[34]

We note that some differences are found with the description of the contact angle evolution made by Xu et al.[32] for their experimental results for this system. In particular, these authors find a critical tilt angle of $\alpha_c \approx 28°$ for the temperature range considered. In addition, as one can observe in Figure 6, the initial experimental values of θ_{max} and θ_{min} are not equal, indicating that the initial contact line is not completely circular. In spite of this, we emphasize that the overall behavior obtained from simulation is very similar to their results.

Finally, we remark that a recent work[28] that presents a new method for evaluating the most stable contact angle of a drop by means of tilting plate experiments is based on the analysis of the dependence on the initial contact angles of α_d and α_u. The simulation method of the present article can also be used for such an analysis, which will be the subject of future work.

SUMMARY

In this work, we have performed a simulation study of the process in which a liquid drop initially placed on a horizontal surface is gradually inclined until it slides. The obtained results have been found to be strongly dependent on the initial contact angle of the drop. In what follows, we present a summary of the main results for each initial condition.

The situation with the initial contact angle equal to θ_{adv} is perhaps the closest to experiments.[18] In this case, the maximum contact angle θ_{max} remains equal to θ_{adv} while θ_{min} decreases with the tilt. Under these circumstances, the front of the drop contact line is displaced downhill while the rear remains fixed. Once θ_{min} attains θ_{rec}, the rear contact line is also displaced but the drop remains static. At critical tilt, most contact angles in the front are equal to θ_{adv}, most contact angles in the rear are equal to θ_{rec}, and the drop slides. For $\theta_{min} > \theta_{rec}$, the total dimensionless retention force is proportional to the cosine difference following eq 17, with a value of k intermediate between 2 and $\pi/2$. For a drop of water of volume $V = 0.056$ cm^3 on an inclined PCTFE surface,[12] we have obtained a value of $k = 1.779$, but our results for other systems show that k can take other values in the range of $\pi/2 < k < 2$ depending on the system size and hysteresis. For $\theta_{min} = \theta_{rec}$, the total dimensionless retention force increases until attaining a critical value slightly smaller than that given by eq 14 (i.e., with a value of k slightly below $k = 2$).

An initial contact angle equal to $\theta_Y = (\theta_{rec} + \theta_{adv})/2$ leads to results previously obtained by finite element methods.[8] In this case, θ_{max} increases and θ_{min} decreases with tilt at a similar rate while the contact line remains fixed. Once θ_{min} (θ_{max}) attains θ_{rec} (θ_{adv}), part of the rear (front) is displaced but the drop remains static. At critical tilt, most contact angles in the rear (front) are equal to θ_{rec} (θ_{adv}), and the drop slides. In accordance with eq 17, for $\theta_{adv} > \theta_{max} > \theta_{min} > \theta_{rec}$, the total dimensionless retention force is proportional to the cosine difference with a slope of $k \approx \pi/2$. Once the maximum cosine difference is attached, the total dimensionless retention force increases toward a critical value characterized by a value of k slightly below 2.

Experimental results for the contact angle evolution are available for molten Sn−Ag−Cu on a tilted oxygen-free Cu substrate.[32] In this case, the experimental initial contact angle is a bit lower than θ_{adv}, and thus one has to deal with a hybrid situation so that for low tilt cos θ_{max} approaches cos θ_{adv} in a linear way while cos θ_{min} increases linearly toward cos θ_{rec}. For higher tilts, $\theta_{max} = \theta_{adv}$ and cos θ_{min} still increase linearly toward cos θ_{rec} but with a different slope. Comparing our simulation results with experimental data shows excellent agreement in spite of being a system with high hysteresis.

To conclude, in this work we have shown that a simulation method based on Surface Evolver can reproduce experimental results for liquid drops on tilted surfaces where contact angle hysteresis gives rise to a capillary retention force that keeps the drop static. Equation 17 establishes a linear relationship between this force and the difference between the cosines of the maximum and minimum contact angles attained by the drop at a given tilt. Furthermore, eqs 18 and 19 show that both cos θ_{max} and cos θ_{min} behave linearly with the sine of the tilt angle.

AUTHOR INFORMATION

Corresponding Author

*E-mail: white@usal.es.

Present Address

†Also at IUFFyM, Universidad de Salamanca, Spain.

Notes

The authors declare no competing financial interest.

ACKNOWLEDGMENTS

We are grateful for financial support by the Ministerio de Educación y Ciencia of Spain under grant FIS2009-07557.

REFERENCES

(1) Young, T. An essay on the cohesion of fluids. *Philos. Trans. R. Soc. London* **1805**, *95*, 65−87.
(2) Laplace, P. S. *Traité de Mécanique Céleste*; Gauthier-Villars: Paris, 1806; Vol. *4*, Supplement to Book 10, p 419.
(3) Macdougall, G.; Ockrent, C. Surface energy relations in liquid/solid systems. I. The adhesion of liquids to solids and a new method of determining the surface tension of liquids. *Proc. R. Soc. London, Ser. A* **1942**, *180*, 151−173.
(4) Bikerman, J. J. Sliding of drops from surfaces of different roughnesses. *J. Colloid Science* **1950**, *5*, 349−359.
(5) Furmidge, C. G. L. Studies at phase interfaces. I. The sliding of liquid drops on solid surfaces and a theory for spray retention. *J. Colloid Science* **1962**, *17*, 309−324.
(6) Larkin, B. K. Numerical solution of the equation of capillarity. *J. Colloid Interface Sci.* **1967**, *23*, 305−312.
(7) Wolfram, E.; Faust, R. Liquid Drops on a Tilted Plate, Contact Angle Hysteresis and the Young Contact Angle. In *Wetting, Spreading and Adhesion*; Padday, J. F., Ed.; Academic Press: London, 1978; pp 213−222.
(8) Brown, R. A.; Orr, F. M.; Scriven, L. E. Static drop on an inclined plate: analysis by the finite element method. *J. Colloid Interface Sci.* **1980**, *73*, 76−87.
(9) Dussan, E.; Chow, R. On the ability of drops or bubbles to stick to non-horizontal surfaces of solids. *J. Fluid Mech.* **1983**, *137*, 1−29.
(10) Dussan, V. On the ability of drops or bubbles to stick to non-horizontal surfaces of solids. Pt. 2: small drops or bubbles having contact angles of arbitrary size. *J. Fluid Mech.* **1985**, *151*, 1−20.
(11) Extrand, C. W.; Gent, A. N. Retention of liquid drops by solid surfaces. *J. Colloid Interface Sci.* **1990**, *138*, 431−442.
(12) Extrand, C. W.; Kumagai, Y. Liquid drops on an inclined plane: the relation between contact angles, drop shape, and retentive force. *J. Colloid Interface Sci.* **1995**, *170*, 515−521.
(13) ElSherbini, A.; Jacobi, A. Retention forces and contact angles for critical liquid drops on non-horizontal surfaces. *J. Colloid Interface Sci.* **2006**, *299*, 841−849.
(14) Bouteau, M.; Cantin, S.; Benhabib, F.; Perrot, F. Sliding behavior of liquid droplets on tilted Langmuir-Blodgett surfaces. *J. Colloid Interface Sci.* **2008**, *317*, 247−254.
(15) Quere, D.; Azzopardi, M.; Delattre, L. Drops at rest on a tilted plane. *Langmuir* **1998**, *14*, 2213−2216.
(16) ElSherbini, A. I.; Jacobi, A. M. Liquid drops on vertical and inclined surfaces: I. An experimental study of drop geometry. *J. Colloid Interface Sci.* **2004**, *273*, 556−565.
(17) ElSherbini, A. I.; Jacobi, A. M. Liquid drops on vertical and inclined surfaces: II. A method for approximating drop shapes. *J. Colloid Interface Sci.* **2004**, *273*, 566−575.
(18) Pierce, E.; Carmona, F.; Amirfazli, A. Understanding of sliding and contact angle results in tilted plate experiments. *Colloids Surf., A* **2008**, *323*, 73−82.
(19) Yadav, P. S.; Bahadur, P.; Tadmor, R.; Chaurasia, K.; Leh, A. Drop retention force as a function of drop size. *Langmuir* **2008**, *24*, 3181−3184.
(20) Tadmor, R.; Yadav, P. As-placed contact angles for sessile drops. *J. Colloid Interface Sci.* **2008**, *317*, 241−246.
(21) Iliev, S. D. Iterative method for the shape of static drops. *Comput. Methods Appl. Mech. Eng.* **1995**, *126*, 251−265.
(22) Iliev, S. D. Static drops on an inclined plane: equilibrium modeling and numerical analysis. *J. Colloid Interface Sci.* **1997**, *194*, 287−300.
(23) Dimitrakopoulos, P.; Higdon, J. On the gravitational displacement of three-dimensional fluid droplets from inclined solid surfaces. *J. Fluid Mech.* **1999**, *395*, 181−209.
(24) Krasovitski, B.; Marmur, A. Drops down the hill: theoretical study of limiting contact angles and the hysteresis range on a tilted plate. *Langmuir* **2005**, *21*, 3881−3885.
(25) Brakke, K. The surface evolver. *Exp. Math.* **1992**, *1*, 141−165.
(26) Santos, M. J.; White, J. A. Theory and simulation of angular hysteresis on planar surfaces. *Langmuir* **2011**, *27*, 14868−14875.
(27) Rodriguez-Valverde, M. A.; Montes Ruiz-Cabello, F. J.; Cabrerizo-Vilchez, M. A. A new method for evaluating the most-stable contact angle using mechanical vibration. *Soft Matter* **2011**, *7*, 53−56.
(28) Ruiz-Cabello, F. J. M.; Rodriguez-Valverde, M. A.; Cabrerizo-Vilchez, M. A new method for evaluating the most stable contact angle using tilting plate experiments. *Soft Matter* **2011**, *7*, 10457−10461.
(29) Tadmor, R. Line energy and the relation between advancing, receding, and young contact angles. *Langmuir* **2004**, *20*, 7659−7664.
(30) Chou, T.-H.; Hong, S.-J.; Sheng, Y.-J.; Tsao, H.-K. Drops sitting on a tilted plate: receding and advancing pinning. *Langmuir* **2012**, *28*, 5158−5166.
(31) Moraila-Martínez, C. L.; Ruiz-Cabello, F. J. M.; Cabrerizo-Vílchez, M. A.; Rodríguez-Valverde, M. A. The effect of contact line dynamics and drop formation on measured values of receding contact angle at very low capillary numbers. *Colloids Surf., A* **2012**, *404*, 63−69.
(32) Xu, H.; Yuan, Z.; Lee, J.; Matsuura, H.; Tsukihashi, F. Contour evolution and sliding behavior of molten Sn-Ag-Cu on tilting Cu and Al_2O_3 substrates. *Colloids Surf., A* **2010**, *359*, 1−5.
(33) Moser, Z.; Gasior, W.; Pstruś, J.; Ksiezarek, S. Surface-tension measurements of the eutectic alloy (Ag-Sn 96.2 at.%) with Cu additions. *J. Electron. Mater.* **2002**, *31*, 1225−1229.
(34) Berejnov, V.; Thorne, R. E. Effect of transient pinning on stability of drops sitting on an inclined plane. *Phys. Rev. E* **2007**, *75*, 066308.